

## WELDING OF HELIUM-DOPED AUSTENITIC AND FERRITIC STAINLESS STEELS

H. T. Lin\*, M. L. Grossbeck\*\*, S. H. Goods<sup>†</sup> and B. A. Chin\*\* Auburn University, \*\* Oak Ridge National Laboratory, <sup>†</sup> Sandia National Laboratories.

CONF-8905118-6

## ABSTRACT

DE89 012523

Helium was uniformly implanted into type 316 stainless steel and Sandvik HT-9 (12Cr-1MoVW) to levels of 0.18 to 256 appm and 0.3 to 1 appm, respectively, using the "tritium trick" technique. Bead-on-plate welds were then produced under fully constrained conditions using the gas tungsten arc (GTA) process. For 316 stainless steel, catastrophic intergranular fracture occurred in the heat-affected zone (HAZ) of welds with helium levels equal to or greater than 2.5 appm. Brittle cracking along the central line of the fusion zone was also observed for the welds containing 105 and 256 appm He. For HT-9, intergranular cracking occurred in the HAZ along prior-austenite grain boundaries of welds containing 1 appm He. Electron microscopy observations showed that the cracking in the HAZ originated from the growth and coalescence of grain boundary helium bubbles and that the fusion zone cracking resulted from the growth of helium at dendrite interfaces. Results of this study indicate that the use of conventional fusion welding techniques to repair irradiation-degraded materials containing even small amounts of helium may be difficult.

EXPOSURE of structural components of nuclear reactors to neutron irradiation will produce significant physical damage to materials and result in the production of helium by  $(n,\alpha)$  reactions [1-4]. Consequently, degradation of mechanical properties and corrosion resistance of the materials will occur. Such deterioration of structural components plays a decisive role in determining the useful life-time of nuclear reactors. Accordingly, it is anticipated that repair and replacement of these degraded components by conventional welding techniques will be required.

To successfully weld neutron-irradiated materials, the behavior of entrapped helium under welding conditions must be understood. It has been known for several decades that the loss of ductility of irradiated materials at elevated temperatures is due to the presence of helium [3]. At high temperatures, helium bubbles grow rapidly under the influence of stress and temperature. As these bubbles coalesce along the grain boundaries, intergranular fracture occurs prematurely. Since welding processes produce internal tensile stresses and high temperatures, entrapped helium may severely affect the weldability and post weld properties of neutron-irradiated materials.

The objective of this research was to provide a scientific background for understanding the effects of helium on weldability and associated problems. To reduce radiological hazards and the need for hot cell operations, helium doping through tritium decay (the "tritium trick" technique) was chosen to evaluate the principal effect of helium on the joining of irradiated materials. This paper presents results for an austenitic stainless steel type 316, and a tempered martensitic steel, HT-9.

## **DISCLAIMER**

**This report was prepared as an account of work sponsored by an agency of the United States Government. Neither the United States Government nor any agency thereof, nor any of their employees, makes any warranty, express or implied, or assumes any legal liability or responsibility for the accuracy, completeness, or usefulness of any information, apparatus, product, or process disclosed, or represents that its use would not infringe privately owned rights. Reference herein to any specific commercial product, process, or service by trade name, trademark, manufacturer, or otherwise does not necessarily constitute or imply its endorsement, recommendation, or favoring by the United States Government or any agency thereof. The views and opinions of authors expressed herein do not necessarily state or reflect those of the United States Government or any agency thereof.**

---

## **DISCLAIMER**

**Portions of this document may be illegible in electronic image products. Images are produced from the best available original document.**

## EXPERIMENTAL PROCEDURES

Austenitic type 316 stainless steel and Sandvik HT-9 were chosen as the base materials for this study. Detailed chemical compositions have been previously published [6]. In this study, type 316 stainless steel was investigated as a primary alloy, and HT-9 was a secondary alloy. The 0.76 mm-thick-plates of type 316 stainless steel were solution-annealed at 1050°C for one hour, while those for HT-9 were solution-annealed at 1050°C for one-half hour followed by a tempering treatment at 750°C for one hour.

The "tritium trick" technique [7] was employed to implant helium into the test materials. In this technique tritium gas is diffused into the material at elevated temperatures. The dissolved tritium is then allowed to decay to form helium by the reaction  $3\text{H} \rightarrow 3\text{He} + \beta^-$  (the half-life of tritium is 12.3 years). All specimens were charged at 300°C for 30 days under tritium pressures ranging from 0.17 to 125 MPa. At the end of this charging period, the exposed materials were removed from the high pressure charging vessel and held at 400°C at 10<sup>-3</sup> Pa in order to remove residual tritium and to stop further generation of helium. To demonstrate that weld defects which occurred during welding arose only from the helium rather than residual tritium, type 316 stainless steel was also charged with hydrogen under the same charging conditions as for the higher helium content specimens. The detailed helium charging conditions for both alloys can be found in ref. [6].

Bead-on-plate GTA welds were made on helium-free and helium-doped materials. For type 316 stainless steel, full-penetration welds were produced in the 0.76-mm-thick plate at 10 V-dc, 24 A at a travel speed of 3.6 mm/s. During welding the plates were fully constrained transverse to the welding direction. HT-9 plates were welded at 10 V-dc, 28 A at a travel speed of 3.6 mm/s under the same constraint conditions as type 316 stainless steel.

Following welding, the as-welded plates were examined in detail using a scanning electron microscope (SEM). The weld microstructures were also examined by preparing metallographic sections transverse to the welding direction. The sections of type 316 stainless steel were electrolytically etched in a solution of 40% HNO<sub>3</sub>- 60% H<sub>2</sub>O. The sections of HT-9 were etched chemically in a solution of 1% HF, 9% HNO<sub>3</sub> and 90% H<sub>2</sub>O. The helium bubble morphology in the heat-affected zone (HAZ) was examined using transmission electron microscopy (TEM).

## RESULTS AND DISCUSSION

### TYPE 316 STAINLESS STEEL

Results of SEM examination and metallography revealed that helium-free plates (control and hydrogen-charged) and plates with the lowest helium content (0.18 appm) were sound and free of weld defects. Specimens with helium contents greater than 0.18 appm all showed significant loss in weldability. Figure 1 shows the representative features of as-welded type 316 stainless steel with the lower (2.5 and 27 appm) and higher (105 and 256 appm) helium concentrations. Severe HAZ cracking was observed in all of the plates with helium levels equal to or greater than 2.5 appm. Typically, HAZ cracking occurred one to three grain diameters from the fusion boundary, and was fully intergranular in nature (Fig. 1a, 1b). At higher helium levels, cracking in the centerline fusion zone was also observed. Since no external stresses were pre-applied, the cracking, in all cases, resulted from the generation of tensile thermal stresses as the constrained plates cooled after the passing of

the welding torch. At higher magnification, the grain facets were observed to be decorated with a uniform distribution of dimples attributed to coalesced helium bubbles (Fig. 1c). The average dimple size was approximately 1  $\mu\text{m}$  and was independent of helium concentration. In addition, the shear ligaments separating the dimples had been rounded by the surface diffusion, indicating that the cracking occurred at high temperature. Video tape recordings showed that HAZ cracking occurred approximately one second after the resolidification of the molten pool.

Figure 2 shows the typical HAZ helium bubble morphology of plates both before and after welding. Generally, the grain boundaries (GBs) of the helium-containing, welded specimens were perforated during the specimen thinning process. This was due to the presence of very large helium bubbles located along the grain boundaries (Fig. 2b). This observation further confirms that dimples on the HAZ cracking surfaces were helium bubbles. Since the helium-free and hydrogen-charged specimens were uncracked, it is clear that the loss of alloy weldability is related to the entrapped helium rather than residual tritium or hydrogen. In addition, the cracking location, one to three grain diameters from the fusion line, suggests that high temperature alone is not sufficient to induce catastrophic intergranular fracture. Rather, a critical combination of high temperature and residual stress controls the bubble growth and fracture process.

The growth of GB helium bubbles is favored by conditions of high temperature and stress. In the case of welding, the high temperatures originate from the welding arc, and tensile stress is generated upon cooling of the constrained plates. The precipitated helium bubbles, which nucleated and formed during the charging period, grew under the actions of high temperature and stress until the reduced contact areas of the grain boundaries could no longer bear the shrinkage-imposed tensile stress, leading to final brittle rupture. The growth kinetics of GB helium bubbles leading to brittle fracture in the HAZ has been developed [8]. The helium cracking model shows that growth of GB helium bubbles is dominated by the stress-induced diffusion of vacancies into bubbles. This bubble growth is first driven by the thermally overpressured gas in the bubbles, and then in turn by the cooling stress. The model predicts that bubbles in grain boundaries one to three grain diameters from the fusion line should reach approximately 0.9  $\mu\text{m}$  in diameter one second after the passing of the torch. The prediction compares favorably with the experimentally measured dimple size (1  $\mu\text{m}$ ) and the onset of cracking.

Fractography of the fusion zone centerline cracking showed that the brittle fracture proceeded along the dendrite boundaries during weld metal resolidification. Visible spherical pores resulting from the migration and coalescence of entrapped helium bubbles in the melt were also observed on the fracture surface. Observations suggest that brittle failure results from the precipitation of helium bubbles at the dendrite interfaces. As solidification proceeds, helium is rejected by the growing dendrites and is trapped between dendrites. These bubbles coalesce into micro-cracks. Shrinkage stresses developed during cooling cause these cracks to propagate, leading to final brittle failure along the center of the fusion zone.

#### MARTENSITIC STEEL

No weld defects were found in the control specimens and in plates with the lowest helium content (0.18 appm). However, the welds of 1 appm He containing material had HAZ weld cracking along the prior-austenite grain boundaries.

This cracking was fully intergranular in nature, as shown in Fig. 3a. At higher magnification the grain facets were observed to be decorated with a uniform distribution of dimples. As in the case of type 316 stainless steel, the cracking had its origin in the growth and coalescence of GB helium bubbles.

## CONCLUSIONS

This study of helium effects on the subsequent weldability of austenitic and ferritic steels led to the following conclusions:

- o Catastrophic intergranular HAZ cracking occurred during cooling of GTA welded type 316 stainless steel and HT-9 with helium levels equal to or greater than about 2.5 and 1 appm, respectively.
- o Brittle fracture in the HAZ of both alloys originates from the growth and coalescence of GB helium bubbles, while brittle fracture in the fusion zone of type 316 stainless steel results from the growth of helium bubbles at dendrite boundaries.
- o Repair of irradiated structural components containing helium levels greater than about 1 appm by conventional GTA welding processes may be difficult.

## Acknowledgments

The authors thank Drs. K. Farrell and R. L. Klueh for reviewing the manuscript. This research was sponsored by the Office of Fusion Energy, U. S. Department of Energy under Contract DE-AC05-84OR21400 with Martin Marietta Energy Systems, Inc., under Contract DE-AC04-76DP00789 with Sandia National Laboratories, Livermore, and by the Division of Materials Sciences, U. S. Department of Energy under the SHaRE program under Contract DE-AC05-76OR00033 with Oak Ridge Associated Universities.

## REFERENCES

1. H. S. Rosenbaum, "Microstructures of Irradiated Materials," Treatise on Materials Science and Technology, Vol. 7, Academic Press, Inc., New York (1975).
2. J. O. Stiegler and L. K. Mansur, "Radiation Effects in Structural Materials," Ann. Rev. Mater. Sci., 9, 405-454 (1979).
3. R. S. Barnes, "Embrittlement of Stainless steels and Nickel-Based Alloys at High Temperature Induced by Neutron Radiation," Nature, 206, 1307-1310 (1965).
4. D. R. Harries, "Neutron Irradiation-Induced Embrittlement in Type 316 and Other Austenitic Steels and Alloys," J. Nucl. Mater., 82, 635-641 (1979).
5. B. A. Chin, R. J. Neuhold and J. L. Straalsund, "Materials Development for Fast Breeder Reactor Cores," Nucl. Technol. 57, 426-435 (1982).
6. H. T. Lin, M. L. Grossbeck, S. H. Goods and B. A. Chin "Degradation in the Weldability of an Austenitic Stainless Steel," to be published in the Proceedings of Effects of Radiation on Materials, ASTM STP 1046.
7. Annual Books and ASTM Standards, "Standard Guide for Simulation of Helium Effects in Irradiated Materials," Vol.12.02, E492-83, pp. 808-811.
8. H. T. Lin, M. L. Grossbeck, S. H. Goods and B. A. Chin "Cavitation Kinetics During GTA Welding of Helium Containing Stainless Steel," submitted to Metallurgical Transaction A.

Fig. 1. Morphological features of as-welded 316 stainless steel. (a) 2.5 appm He welds show HAZ intergranular fracture, (b) 105 appm He welds show brittle fracture in HAZ and fusion zone, and (c) SEM micrographs of grain boundary facets decorated with a uniform distribution of dimples.

Fig. 2. TEM micrographs showing grain boundary helium bubbles of 316 stainless steel. (a) Helium bubble microstructure before welding, and (b) perforated grain boundary in the HAZ due to growth and coalescence of grain boundary helium bubbles.

Fig. 3. Structure of as-welded HT-9 with 1 appm He. (a) Intergranular fracture along prior-austenite grain boundaries, and (b) grain boundary facets decorated with a uniform distribution of dimples.

## DISCLAIMER

This report was prepared as an account of work sponsored by an agency of the United States Government. Neither the United States Government nor any agency thereof, nor any of their employees, makes any warranty, express or implied, or assumes any legal liability or responsibility for the accuracy, completeness, or usefulness of any information, apparatus, product, or process disclosed, or represents that its use would not infringe privately owned rights. Reference herein to any specific commercial product, process, or service by trade name, trademark, manufacturer, or otherwise does not necessarily constitute or imply its endorsement, recommendation, or favoring by the United States Government or any agency thereof. The views and opinions of authors expressed herein do not necessarily state or reflect those of the United States Government or any agency thereof.

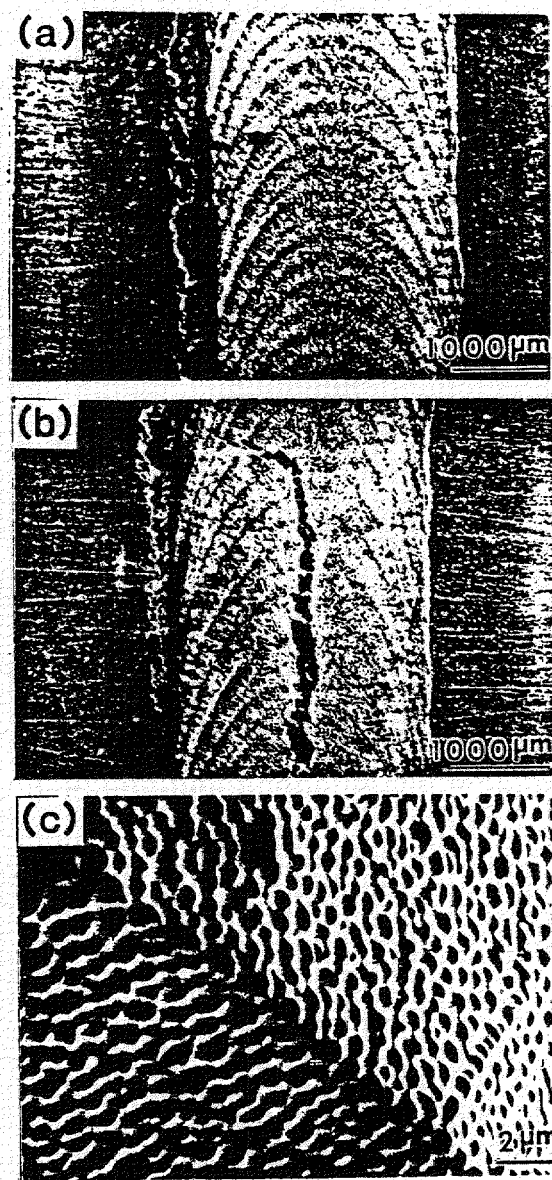


Figure 1

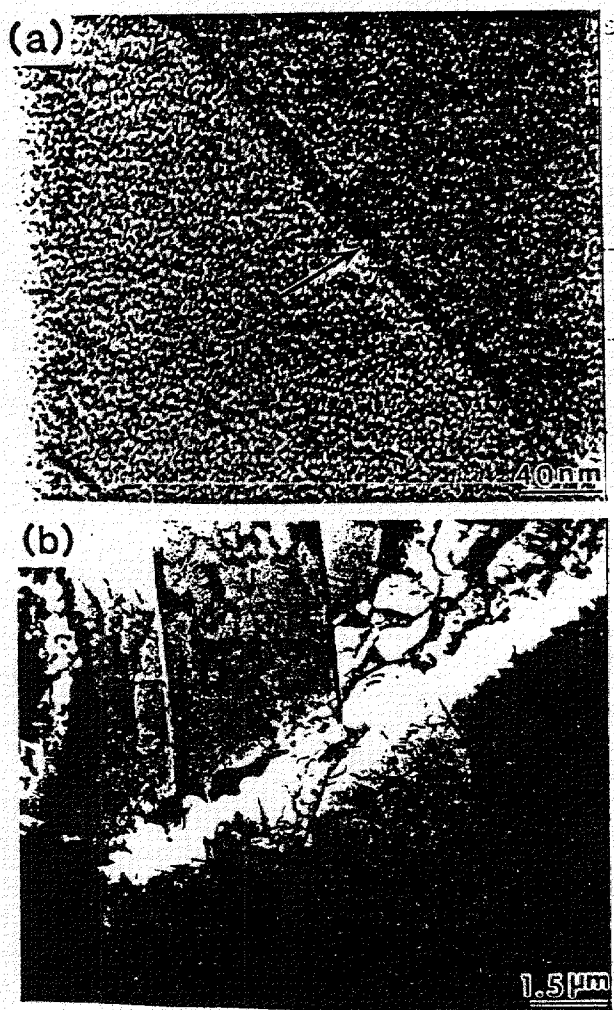


Figure 2

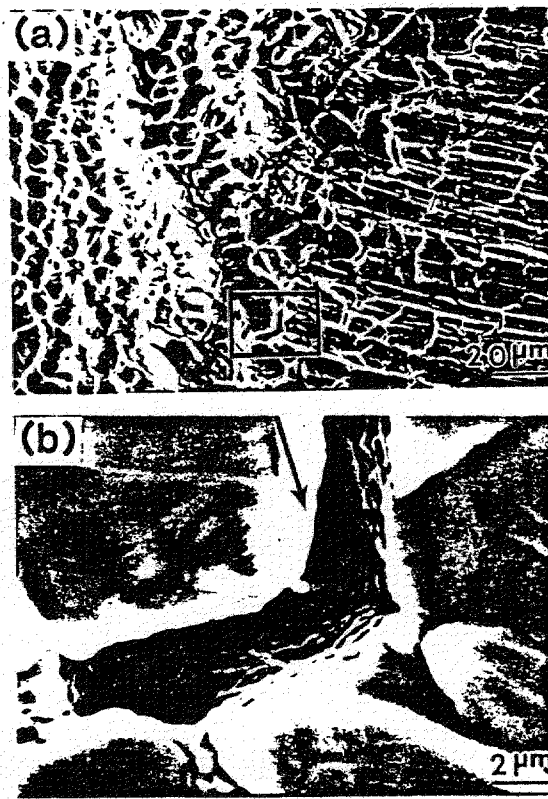


Figure 3